MAGNET DEVELOPMENT FOR THE BRF POSITRON EMISSION TOMOGRAPHY ACCELERATOR

N. Chester, A. Makarov, P. Schlabach, I. Terechkine,
D. Walbridge, T. Wokas, V. Yarba
Fermi National Accelerator Laboratory*
D.J. Larson
Science Applications International Corporation

Abstract

A collaboration involving the Biomedical Research Foundation, Science Applications International Corporation, Fermi National Accelerator Laboratory, and the University of Washington is developing an accelerator for producing isotopes for Positron Emission Tomography (PET) scans. The Medium Energy Beam Transport (MEBT) section of this accelerator takes a small beam from a first RFQ acceleration device and matches it into a small 3D-acceptance at a second RFQ section. The beam transport system was designed to prevent beam losses due to emittance growth. The system includes two bending dipoles and seven quadrupoles of three different types.

This report contains a brief description of the MEBT magnets and their electric, magnetic and thermal properties. The magnet measurements show that each of the magnets meets the system requirements.

1 INTRODUCTION

The alternative method of isotope production for PET scans uses Radio-Frequency Sections to accelerate $3He^{++}$ particles up to 10.5 MeV [1]. The linac transport system consists of low energy, medium energy, and high energy parts. One 1 MeV, 212.5 MHz RFQ section and three 425 MHz RFQ sections bring the beam energy up to the target 10.5 MeV value. The MEBT, medium energy part of the accelerator (figure 1), is designed
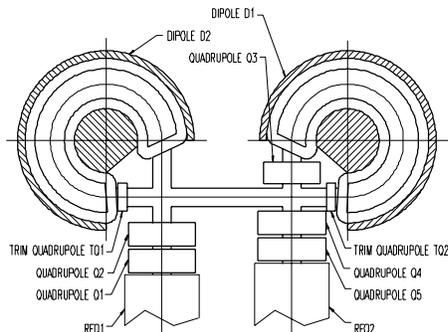

Figure 1. PET MEBT layout.

_____

to accept the beam from the first RFQ section and insure proper beam transverse size and desired bunch longitudinal size at the entrance aperture of the second RFQ section. System requirements and space limitations resulted in a specific design for the bending dipoles and for each of the three quadrupole types used in the MEBT.

2 BENDING GRADIENT DIPOLES

Two 270° gradient dipoles were inserted into the MEBT to allow magnetic rebunching between the first and the second RFQ sections, and to reduce the accelerator length. The dipoles have a central line radius R = 304.8 mm, a pole width w = 158.75 mm, and a central line pole gap g = 30.48 mm. The central line, central plane (plane of symmetry) magnetic field required for the transportation of 1.0 MeV $3He^{++}$ particles is $B_0 = 4101$ G, but the dipoles were designed to allow $B_0 = 8202$ G to have a possibility for $3He^{+}$ ion transportation through the MEBT channel. The magnetic field has to be a linear function of radius with field index **n** at central line (R = R_0)

$$n = -\frac{R_0}{B_0} \cdot \frac{dB}{dR} = 0.53.$$

The magnet pole ends were shaped for additional focusing to reduce the number of required additional focusing devices. The two magnets used in the MEBT system are identical except for their mirror symmetry. The magnet main parameters are listed below:

- diameter and height - ∅0.96 m x 0.33 m;
- weight - 1400 kg;
- wire used - 5.79 mm square wire with ∅ 3.2 mm hole for cooling water;
- total number of turns per magnet - 112;
- maximum current - 180 A ($B_0 = 8202$ G);
- nominal wire resistance at 20° C - 0.270 Ohm;
- calculated low-frequency inductance - 0.12 H;
- maximum power losses at 180 A - 9300 W;
- water temperature rise at 180 A - 30° C;
- minimum water flow required at 180 A - 4.6 l/min.;
- number of parallel water circuits per magnet - 8;

For proper system operation, only ±3.2 G difference is allowed between the real and ideal magnetic field in a

region **254 mm < R < 355 mm** at nominal field strength.

A tolerance analysis made using the OPERA-2D program has shown that in order to meet this requirement, it is necessary to machine the magnet pole surfaces with an accuracy of about 10 μm. Figure 2 shows the difference between the measured (or calculated) and ideal magnetic field that is plotted against the radial position. Calculations were based on the measured pole profile.
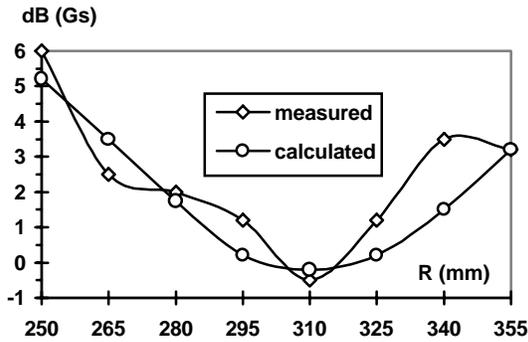

Figure 2. The Dipole Field Quality. B_0=8200 G.

The dipole excitation curve is practically a linear function of current, but about 100 G magnetic field hysteresis exists.

3 QUADRUPOLES

The MEBT quadrupoles focus the beam transverse dimensions inside an allowed range at the entrance into the dipole D1 and into the RFQ-2 (figure 1). Five main and two trim quadrupoles are installed in the MEBT beam-line. Table 1 below shows the required integrated strength for the main quadrupoles.

Table 1

	Q1	Q2	Q3	Q4	Q5
G*L (T)	0.72	0.66	0.15	0.92	1.28

All quadrupoles should have an aperture R≥38 mm. The length of the main quadrupoles must be less than 125 mm. The width of Q1, Q2, Q4, and Q5 can't be larger than 400 mm; the width of Q3 should be less than 300 mm. Trim quadrupoles should have minimum integrated strength G*L = 0.04 T, their length should not exceed 50 mm and width - 150 mm. Because of the relatively large integrated strength of Q1, Q2, Q4, and Q5, only water-cooled coils can be used. Trim quadrupoles and Q3 were made with air-cooled coils.

3.1 Water-cooled quadrupoles

The cores for the Q1, Q2, Q4, and Q5 quadrupoles were made from the laminations that were used for the Fermilab 3Q-120 quadrupole production in the 1980's.

To meet the integrated strength requirements the core length was chosen equal to 50 mm.

The main water-cooled quadrupole parameters are listed below:

wire used - 5.79 mm square wire with ∅ 3.2 mm hole for cooling water;

number of turns per pole - 48;

nominal quadrupole resistance - 0.04675 Ohm;

low-frequency magnet inductance - 7 mH;

power losses at integrated strength 1.3 T - 5000 W;

minimum water flow required - 1.2 liter/min.

temperature rise at minimum water flow - 60° C;

number of parallel water circuits per magnet - 2.

Figure 3 shows the difference between the calculated and ideal magnetic field, which is a linear function of X, for the gradient G = 2000 G/cm corresponding to the integrated strength required for the Q5 quadrupole.
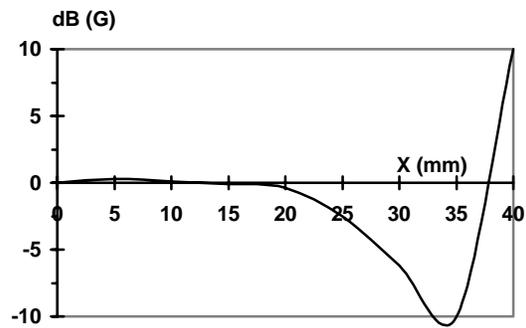

Figure 3. Water-cooled quadrupole field quality.

As the quadrupole excitation curve (figure 4) shows, the current required to achieve the Q5 maximum integrated strength (table 1) is about 1.7 times larger than that for the quadrupole with an ideal core.
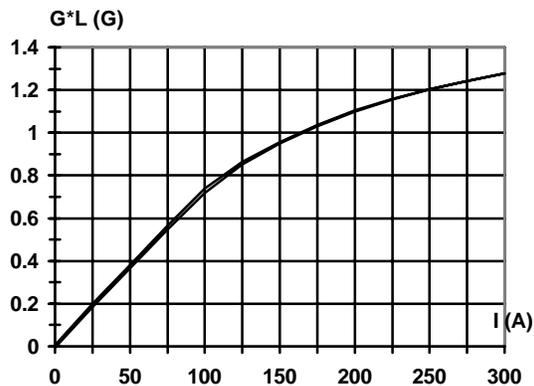

Figure 4. Q5 quadrupole excitation curve.

2D magnetic modeling can explain only 30% of the current rise due to the steel nonlinearity. This difference originates from the very short length of the quadrupole: the end flux of the quadrupole becomes comparable with the useful flux. The problem can be corrected by

making the pole tip length as large as possible within the allowed quadrupole total length limit.

3.2 Air-cooled quadrupoles

Except for required maximum field strength and dimensions, Q3 and the trim quadrupoles have a similar design (figure 5).
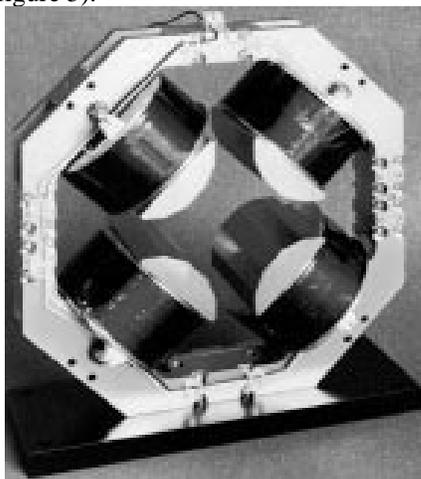

Figure 5. Air-cooled Quadrupole.

To make air-cooling possible, the pole length was made as large as the space limitation allowed. Poles were manufactured from solid steel; flux returns were assembled from two halves to allow quadrupole mounting around the PET beam-pipe. Coils were wound on cylindrical bobbins using solid round insulated copper wire. Coil-pole assemblies were mounted into a flux return frame using assembly tooling that insured proper pole positioning. The main design parameters for the trim quadrupoles are listed below:

    wire - film coated $\varnothing$ 0.7 mm round copper wire;
    number of turns per coil - 315;
    quadrupole resistance - 7.0 Ohm;
    nominal current - 1.1 A;
    quadrupole low-frequency inductance - 0.2 H;
    power losses at nominal current - 9.0 W;
    maximum coil current allowed - 3.0 A;
    surface temperature at maximum current - 95° C.

Figure 6 shows the excitation properties of the trim quadrupole. Analysis of this excitation curve reveals a significant reserve in the integrated strength, but this reserve is too small to use a trim quadrupole instead of Q3. The Q3 quadrupole has a larger length and steel cross-section in order to meet the integrated strength requirement. The design parameters for Q3 are listed below:

    wire - film coated $\varnothing$ 1.15 mm round copper wire;
    number of turns per coil - 1190;
    quadrupole resistance - 19.1 Ohm;
    nominal current - 0.64 A;
    quadrupole low-frequency inductance - 6.7 H;
    power losses at nominal current - 8.0 W;

maximum coil current allowed - 4.0 A;
surface temperature at maximum current - 95° C

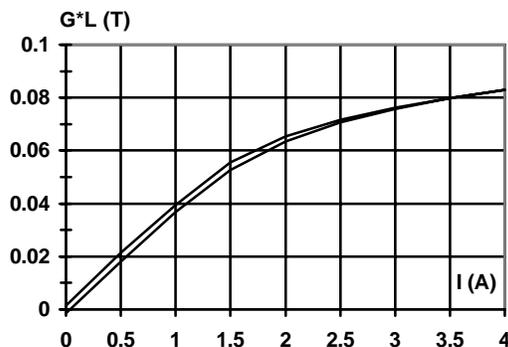The excitation curve for Q3 is shown in figure 7.
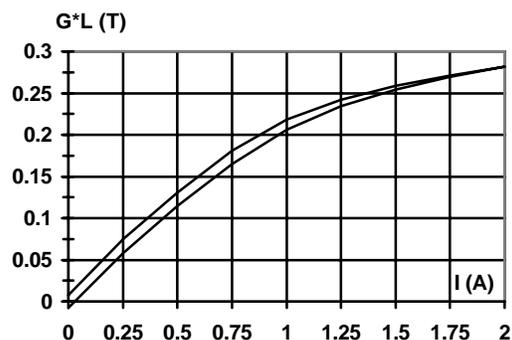

Figure 6. Trim quadrupole excitation curve.

Figure 7. Q3 quadrupole excitation curve.

4 CONCLUSION

A set of magnetic devices was designed, manufactured and tested at Fermilab for the PET Medium Energy Beam Transport System. The magnets' properties are close to what was expected. The recent PET accelerator beam experiments [2] have shown that the MEBT meets the system requirements.

References.

1. D.J. Larson, P.E. Young, D Sun, at al.,
Ion Optical Design of the BRF-FNAL-SAIC-UW PET Accelerator. PAC-97, 4V.18.
2. Ralph Pasquinelli,
A 3He^{++} RFQ Accelerator for the Production of PET Isotopes. PAC-97, 9B.09